

On field-driven domain wall motion in compensated ferrimagnetic nanowires

K. Y. Jing,¹ X. Gong,¹ and X. R. Wang^{1,2,*}

¹Physics Department, The Hong Kong University of Science and Technology, Clear Water Bay, Kowloon, Hong Kong

²HKUST Shenzhen Research Institute, Shenzhen 518057, China

(Dated: August 2, 2022)

The fascinating high-speed field-driven domain wall (DW) motion along ferrimagnetic nanowires near the angular momentum compensation point (AMCP) is solved based on the generic ferrimagnetic dynamics. The physics of the absences of precessional torque and infinite high Walker breakdown field at the AMCP is proved under general conditions. Based on the energy conservation principle, an almost exact DW velocity formula, valid beyond the Walker breakdown field, is obtained. Our results agree with all existing experiments and simulations. This theory provides useful guidances to DW manipulation.

Introduction.— Magnetic domain wall (DW) dynamics in nanowires have attracted much attention for its rich physics [1, 2] and promising device applications such as racetrack memories [3]. One critical issue in applications is the realization of high stable DW speed under external forces such as magnetic fields and electrical currents. This requires a delay or removal of so-called Walker breakdown [4]. The endeavour of increasing DW speed leads to studying DW motion in antiferromagnetic nanowires [5–7], and, very recently, to that in ferrimagnetic nanowires [8–19]. A ferrimagnet has at least two spin sublattices antiferromagnetically interacting with each other. It has two special states called the angular momentum compensation point (AMCP) at which the angular momenta of the two sublattices cancel each other and the magnetization compensation point at which the magnetizations cancel each other. One class of ferrimagnets is rare-earth-transition-metal alloys whose AMCP and magnetization compensation point are different in general and can be tuned by compositions, other than the temperature. Unlike an antiferromagnet, ferrimagnetic states can be manipulated by a magnetic field, a spin transfer torque, and a spin-orbit torque. Also, unlike a ferromagnet, the net magnetization of a ferrimagnet can be very small but not zero, especially around an AMCP such that it is susceptible to the magnetic field with small Zeeman energy. One fascinating discovery is the very high DW speed of thousands meters per second in compensated ferrimagnetic (FiM) nanowires near the AMCP [9–11]. Here we show that high DW speed near the AMCP is related to the absence of precessional torque and Walker breakdown phenomenon at the AMCP.

Although FiM dynamics should be described by coupled partial differential equations for magnetizations on at least two antiferromagnetically coupled sublattices, existing theoretical studies treat a ferrimagnet either as a ferromagnet whose dynamics follows Landau-Lifshitz-Gilbert (LLG) equation [10, 11] or an antiferromagnet with the Néel order governed by a second-order partial differential equation [9, 12, 16, 20–22]. DW dynamics is then obtained from converting the partial differential equations into ordinary differential equations for the collective coordinates of DW center and DW-plane canting angle [9, 12, 16, 20–22]. Indeed, existing theories have enriched our understanding of DW dynamics in ferri-

magnets in many aspects. However, there are some drawbacks in these approaches. These approaches fail to provide a quantitative explanation to both experiments and simulations since they rely on the existence of a DW plane and a rigid body assumption for the Thiele equation [23]. It often needs to assume also certain DW structure such that the approaches are difficult, if not impossible, to generalize to situations where the assumptions are not valid such as for vortex DWs and DWs in chiral magnets. Furthermore, the physical picture behind the FiM DW motion is unclear in these approaches and an accurate description of the DW speed beyond the Walker breakdown field is still challenging.

In this work, the origin of the high DW speed and absence of Walker breakdown field at the AMCP of a FiM nanowire are explained based on generic dynamics for coupled sublattice magnetizations of a ferrimagnet with a general Rayleigh dissipation. We show that a static DW between two domains with different energy densities does not exist. Spins in the DW must move in a field that creates such an energy density difference. Moving spins must dissipate energy due to the inevitable coupling between spins and its environment described by Gilbert damping in magnetization dynamics. The dissipated energy must be compensated by the Zeeman energy released from the DW propagation toward domain of the higher energy density. At the AMCP, precessional torque vanishes due to the zero angular momentum and the Walker breakdown field become infinity, leading to the high DW speed. Furthermore, a universal relationship between DW speed and DW structure is obtained, and an almost exact formula for high-field DW velocity is derived.

Model.— We consider a head-to-head (HH) DW in a FiM nanowire, whose easy axis is along the wire defined as the z -axis as shown in Fig. 1. \mathbf{M}_1 and \mathbf{M}_2 are the magnetizations on two sublattices with M_1 and M_2 being their saturation magnetization. The total magnetic energy of the wire in the presence of a uniform magnetic field \mathbf{H} is $E = \int \varepsilon d^3x$ with the energy density of

$$\varepsilon = J\mathbf{M}_1 \cdot \mathbf{M}_2 + \sum_{i=1,2} \left[A_i (\nabla \mathbf{M}_i)^2 + f_i(\mathbf{M}_i) - \mu_0 \mathbf{M}_i \cdot \mathbf{H} \right], \quad (1)$$

where $J > 0$ is the antiferromagnetic interlattice-spin coupling constant. A_i and f_i are the ferromagnetic exchange stiffness

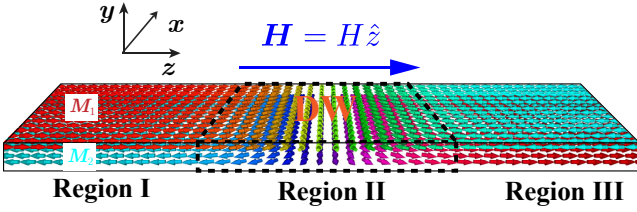


FIG. 1. Schematic of a HH FiM DW in a nanowire. Region I and III are two uniform FiM domains, separated by a DW (region II) whose width is Δ . DW structure can be very complicated. \mathbf{H} is the external field. Colours denote the spin orientations: The red for spins along \hat{z} and the light-blue for spins along $-\hat{z}$.

and anisotropic magnetic energy density for sublattice i ($i = 1, 2$). f_i is assumed to have two equal minima at $\mathbf{M}_i = \pm M_i \hat{z}$.

The FiM magnetization dynamics is generically governed by the following equations [24, 25]

$$\begin{aligned} \frac{1}{\gamma_1} \frac{\partial \mathbf{M}_1}{\partial t} &= -\mathbf{M}_1 \times \left(\mathbf{H}_1 - \frac{\alpha_{11}}{\gamma_1 M_1} \frac{\partial \mathbf{M}_1}{\partial t} - \frac{\alpha_{12}}{\gamma_1 M_1} \frac{\partial \mathbf{M}_2}{\partial t} \right) \\ \frac{1}{\gamma_2} \frac{\partial \mathbf{M}_2}{\partial t} &= -\mathbf{M}_2 \times \left(\mathbf{H}_2 - \frac{\alpha_{22}}{\gamma_2 M_2} \frac{\partial \mathbf{M}_2}{\partial t} - \frac{\alpha_{21}}{\gamma_2 M_2} \frac{\partial \mathbf{M}_1}{\partial t} \right), \end{aligned} \quad (2)$$

where $\mathbf{H}_i = -\mu_0^{-1} \delta E / \delta \mathbf{M}_i$ and $\gamma_i = g_i \mu_B / \hbar$ ($i = 1, 2$) are the effective field and the gyromagnetic ratio for \mathbf{M}_i , respectively. g_i , μ_B , and \hbar are the Landé g -factor of sublattice i ($i = 1, 2$), the Bohr magneton, and the Planck constant, respectively. α_{11} , α_{22} and α_{12} , α_{21} are intra-sublattice and inter-sublattice damping coefficients. We have $\frac{\alpha_{12}}{\gamma_1 M_1} = \frac{\alpha_{21}}{\gamma_2 M_2}$ due to the action-reaction law. $s_i = M_i / \gamma_i$ is the spin density of sublattice i ($i = 1, 2$). $\gamma_1 \neq \gamma_2$ in a general ferrimagnet because of the difference in Landé g -factors of sublattices. For example, in GdFeCo alloys, $g_{\text{Gd}} \approx 2$, $g_{\text{FeCo}} \approx 2.2$ [9].

Results.— We prove first that no static DW is allowed in the presence of a magnetic field along the z -direction, except at magnetization compensation point. If a static DW solution exists, the DW structure should satisfy equations $\mathbf{M}_i \times \mathbf{H}_i = 0$ ($i = 1, 2$). As illustrated in the Supplemental Materials [26], it implies $\mathbf{M}_i(\mathbf{x}, t)$ ($i = 1, 2$) satisfying following equation

$$\oint_{\partial \Omega} \left[\varepsilon \mathbb{1} - \sum_{i=1,2}^{j=x,y,z} 2A_i (\nabla M_{i,j}) \otimes (\nabla M_{i,j}) \right] \cdot d\boldsymbol{\sigma} = \text{const.} \quad (3)$$

where $\partial \Omega$ is any closed surface of the system, $\mathbb{1}$ is the 3×3 unit matrix, and \otimes denotes the dyadic product. Eq. (3) cannot be true for a DW with $\mathbf{M}_1 = M_1 \hat{z}$, $\mathbf{M}_2 = -M_2 \hat{z}$ on its left and $\mathbf{M}_1 = -M_1 \hat{z}$, $\mathbf{M}_2 = M_2 \hat{z}$ on its right as shown in Fig. 1, or vice versa, because it requires $(M_1 - M_2)H = 0$. Thus, a static DW can only exist either with $H = 0$ or $M_1 = M_2$. In other words, a static DW cannot exist between two domains with different energy density. This result can also be understood from following argument: Assume $\mathbf{M}_i(\mathbf{x})$ is a static DW that separate a left domain with a lower energy density ε_1 from the right domain with a higher energy density $\varepsilon_2 (> \varepsilon_1)$. The energy change by shifting DW to the right by a distance L , i.e.

$\mathbf{M}_i(\mathbf{x}) \rightarrow \mathbf{M}_i(\mathbf{x} + L\hat{z})$, is $LS(\varepsilon_1 - \varepsilon_2) < 0$, here S is the cross section area of the wire. The DW is not stable against a rigid shift to the right because this small change in spin structure always lower the system energy. Thus a DW must vary with time under a magnetic field.

When J is much larger than the Zeeman energy, \mathbf{M}_1 and \mathbf{M}_2 are always anti-parallel to each other. We define $\mathbf{M}_{\text{eff}} = (M_1 - M_2)\mathbf{m}$, where \mathbf{m} is the unit vector of \mathbf{M}_1 . Then \mathbf{m} satisfies the following equation

$$(s_1 - s_2) \frac{\partial \mathbf{m}}{\partial t} = -(M_1 - M_2) \mathbf{m} \times \mathbf{H}_{\text{eff}} + \alpha \mathbf{m} \times \frac{\partial \mathbf{m}}{\partial t}, \quad (4)$$

where $\mathbf{H}_{\text{eff}} = \frac{M_1 \mathbf{H}_1 - M_2 \mathbf{H}_2}{M_1 - M_2}$. In terms of \mathbf{m} , the total energy is $E[\mathbf{m}] = \int [A(\nabla \mathbf{m})^2 + f(\mathbf{m}) - \mu_0(M_1 - M_2)\mathbf{m} \cdot \mathbf{H}] d^3 \mathbf{x}$ with $A = A_1 M_1^2 + A_2 M_2^2$, where a is the lattice constant. Denote $\alpha = \alpha_{11} s_1 + \alpha_{22} s_2 - \alpha_{12} s_2 \frac{\gamma_2}{\gamma_1} - \alpha_{21} s_1 \frac{\gamma_1}{\gamma_2}$, the thermodynamic second law requires $\alpha > 0$ to ensure the Rayleigh dissipation functional $\mathcal{R} = \frac{\mu_0 \alpha}{2} \int \left(\frac{\partial \mathbf{m}}{\partial t} \right)^2 d^3 \mathbf{x}$ [24, 25, 27] to be positive-definite. Equation (4) says that the change of spin angular momentum (left-hand side) equals the net torque (right-hand side) that is the sum of a torque from an effective field on the net magnetization ($M_1 - M_2 \neq 0$) and a dissipative torque from the motion of \mathbf{m} . At the AMCP, the dissipative torque cancels the field torque.

Equation (4) can be recast as an effective LLG equation [11, 20, 28–30]

$$\frac{\partial \mathbf{m}}{\partial t} = -\gamma_{\text{eff}} \mathbf{m} \times \mathbf{H}_{\text{eff}} + \alpha_{\text{eff}} \mathbf{m} \times \frac{\partial \mathbf{m}}{\partial t}, \quad (5)$$

with an effective gyromagnetic ratio $\gamma_{\text{eff}} = |M_1 - M_2| / (s_1 - s_2)$ and an effective Gilbert damping $\alpha_{\text{eff}} = \alpha / (s_1 - s_2)$. $\gamma_{\text{eff}} \alpha_{\text{eff}}$ is always positive because a moving magnetization must dissipate its energy to its environment (See Eq. (6) below). $s_1 > s_2$ and $s_1 < s_2$ correspond to lattice-1 and lattice-2 dominate cases. Following a similar derivation in the literature [31, 32], the energy dissipation rate is [33, 34],

$$\frac{dE}{dt} = -\frac{\alpha_{\text{eff}} \gamma_{\text{eff}} \mu_0}{(1 + \alpha_{\text{eff}}^2)(M_1 - M_2)} \int (\mathbf{M}_{\text{eff}} \times \mathbf{H}_{\text{eff}})^2 d^3 \mathbf{x}. \quad (6)$$

We divide the wire into three regions as shown in Fig. 1: I for the domain with \mathbf{M}_{eff} parallel to \mathbf{H} , II for the DW, and III for the domain with \mathbf{M}_{eff} anti-parallel to \mathbf{H} . Energy dissipation occurs only in the DW region (region II) where \mathbf{M}_{eff} and \mathbf{H}_{eff} are not collinear [33, 34]. The change of energies, E_I and E_{III} , of region I and III comes from the DW propagation along the wire, and should be $\frac{d(E_I + E_{III})}{dt} = -2\mu_0(M_1 - M_2)HvS$, where v is the DW velocity. DW energy E_{II} must be around a certain value. Thus the time averaged energy change rate must be zero. In another word, $\frac{dE_{II}}{dt}$ is either zero or oscillates with zero average. The energy conservation requires

$$\begin{aligned} v &= \frac{\alpha_{\text{eff}} \gamma_{\text{eff}}}{2HS(1 + \alpha_{\text{eff}}^2)} \int (\mathbf{m} \times \mathbf{H}_{\text{eff}})^2 d^3 \mathbf{x} \\ &+ \frac{1}{2\mu_0(M_1 - M_2)HS} \frac{dE_{II}}{dt}. \end{aligned} \quad (7)$$

This is a universal relationship between DW velocity and the DW structure and can serve as a proper definition of instantaneous DW velocity. The second term on the right should be identical zero in the case of a rigid DW motion such that the DW speed is constant. In the case that a DW deforms itself during its propagation, the energy dissipation rate and DW energy E_{\parallel} oscillate with time and $\frac{dE_{\parallel}}{dt} = 0$, where the bar denotes the time average. This results in an oscillating DW speed whose time-averaged value is

$$\bar{v} = \frac{\alpha_{\text{eff}}\gamma_{\text{eff}}}{2HS(1+\alpha_{\text{eff}}^2)} \int (\mathbf{m} \times \mathbf{H}_{\text{eff}})^2 d^3\mathbf{x}. \quad (8)$$

We note $(\mathbf{m} \times \mathbf{H}_{\text{eff}})^2 = H_{\text{eff},\theta}^2 + H_{\text{eff},\phi}^2$, where $H_{\text{eff},\theta}$ and $H_{\text{eff},\phi}$ are two field components perpendicular to \mathbf{m} in the local coordinate framework $(\mathbf{e}_m, \mathbf{e}_\theta, \mathbf{e}_\phi)$. $\theta(\mathbf{x}, t)$ and $\phi(\mathbf{x}, t)$ are the polar and the azimuthal angles of \mathbf{m} . Below we consider anisotropy energy of $f(\mathbf{m}) = -K_z m_z^2 + K_y m_y^2$.

$$\begin{aligned} H_{\text{eff},\theta} &= H \sin \theta - G, \\ H_{\text{eff},\phi} &= -\frac{1}{\mu_0(M_1 - M_2) \sin \theta} \frac{\partial f}{\partial \phi} \\ &\quad + \frac{2A}{\mu_0(M_1 - M_2) \sin \theta} \frac{\partial}{\partial z} \left(\sin^2 \theta \frac{\partial \phi}{\partial z} \right), \end{aligned} \quad (9)$$

where $G = \frac{1}{\mu_0(M_1 - M_2)} \left[2A \frac{\partial^2 \theta}{\partial z^2} - \frac{\partial f}{\partial \theta} - 2A \sin \theta \cos \theta \left(\frac{\partial \phi}{\partial z} \right)^2 \right]$.

Equation (5) along $\mathbf{e}_\theta, \mathbf{e}_\phi$ becomes

$$\begin{aligned} \frac{\partial \theta}{\partial t} &= \gamma_{\text{eff}} H_{\text{eff},\phi} - \alpha_{\text{eff}} \sin \theta \frac{\partial \phi}{\partial t} \\ \sin \theta \frac{\partial \phi}{\partial t} &= -\gamma_{\text{eff}} H_{\text{eff},\theta} + \alpha_{\text{eff}} \frac{\partial \theta}{\partial t}. \end{aligned} \quad (10)$$

Eliminate time-derivative of θ from equation (10), we have

$$(1 + \alpha_{\text{eff}}^2) \sin \theta \frac{\partial \phi}{\partial t} = \gamma_{\text{eff}} (\alpha_{\text{eff}} H_{\text{eff},\phi} - H_{\text{eff},\theta}). \quad (11)$$

If the DW propagates as a rigid-body along the z -direction, the case of a field below the Walker breakdown [4], i.e. $\frac{\partial \phi}{\partial z} = 0$, $\frac{\partial^2 \phi}{\partial z^2} = 0$, and $\frac{\partial \phi}{\partial t} = 0$, using Eq. (9), we have $2A \frac{\partial^2 \theta}{\partial z^2} - \frac{\partial f}{\partial \theta} = 0$, so that $H_{\text{eff},\theta} = -H \sin \theta$, whose maximal allowed external field is the Walker breakdown field. For $(M_1 - M_2), (s_1 - s_2) \neq 0$, $\frac{\partial \phi}{\partial t} = 0$ obviously requires $\alpha_{\text{eff}} H_{\text{eff},\phi} = H_{\text{eff},\theta}$. This means that the DW-plane cants an angle to generate a non-zero $H_{\text{eff},\phi}$ to coherently vary θ such that the DW propagates along the wire. Recall our biaxial model $f(\theta, \phi) = -K_z \cos^2 \theta + K_y \sin^2 \theta \sin^2 \phi$, the Walker breakdown field is $H_W = \max \left(\frac{\alpha_{\text{eff}} K_y \sin 2\phi}{\mu_0(M_1 - M_2)} \right) = \frac{\alpha K_y}{\mu_0(M_1 - M_2)(s_1 - s_2)}$. Both γ_{eff} and α_{eff} diverge as $(s_1 - s_2)^{-1}$ near the AMCP. The limit of Eq. (11) under $s_1 - s_2 \rightarrow 0$ ($\alpha_{\text{eff}}^2, \gamma_{\text{eff}} \alpha_{\text{eff}} \sim (s_1 - s_2)^{-2}$) gives $H_{\text{eff},\phi} = 0$ and $\phi = 0$ when $\frac{\partial \phi}{\partial t} = 0$. Thus the DW-plane remains in the xz -plane and never rotates, leading to an infinite H_W at the AMCP. One can also see this point by considering an equivalent form of Eq. (5), $\frac{\partial \mathbf{m}}{\partial t} = -\frac{\gamma_{\text{eff}}}{1 + \alpha_{\text{eff}}^2} \mathbf{m} \times \mathbf{H}_{\text{eff}} -$

$\frac{\gamma_{\text{eff}} \alpha_{\text{eff}}}{1 + \alpha_{\text{eff}}^2} \mathbf{m} \times (\mathbf{m} \times \mathbf{H}_{\text{eff}})$. At the AMCP, the precessional torque vanishes since $\frac{\gamma_{\text{eff}}}{1 + \alpha_{\text{eff}}^2} \rightarrow 0$ as $(s_1 - s_2) \rightarrow 0$ while the damping torque is finite because of $\lim_{(s_1 - s_2) \rightarrow 0} \frac{\gamma_{\text{eff}} \alpha_{\text{eff}}}{1 + \alpha_{\text{eff}}^2} = \frac{M_1 - M_2}{\alpha} \neq 0$. This means that the precessional motion is completely prohibited, and \mathbf{m} at any point inside the DW rotates coherently toward external field, leading to a rigid DW propagation along the wire (see the Supplemental Materials [26]).

Equation (5) with our biaxial magnetic anisotropy has the well-known Walker DW solution [4] of $\theta(z, t) = 2 \arctan \left(\exp \left((z - \int_0^t v(\tau) d\tau) / \Delta(t) \right) \right)$, where Δ is the DW width. It gives $\frac{dE_{\parallel}}{dt} = -\frac{4AS}{\Delta^2} \frac{d\Delta}{dt} = 0$ for a rigid-body DW propagation. $H_{\text{eff},\theta} = \alpha_{\text{eff}} H_{\text{eff},\phi} = -H \sin \theta$, $(\mathbf{m} \times \mathbf{H}_{\text{eff}})^2 = H_{\text{eff},\theta}^2 + H_{\text{eff},\phi}^2 = (1 + \alpha_{\text{eff}}^2) H^2 \sin^2 \theta / \alpha_{\text{eff}}^2$. Substituting DW width definition of $\int \sin^2 \theta d^3\mathbf{x} = 2S\Delta$ into Eq. (7), one has $v = \frac{(M_1 - M_2)\Delta}{\mu_0(M_1 - M_2)} H$ and DW speed at Walker breakdown field $v_W = \frac{\alpha K_y \Delta}{\mu_0(s_1 - s_2)}$, independent of the damping coefficient and divergent at the AMCP.

Away from the AMCP, H_W is finite. A DW shall precess around wire axis while it propagates along the wire when $H > H_W$. From Eqs. (8) and (9), we have

$$\bar{v} = \frac{\alpha_{\text{eff}} \gamma_{\text{eff}}}{2HS(1 + \alpha_{\text{eff}}^2)} \int \left[(H \sin \theta - G)^2 + H_{\text{eff},\phi}^2 \right] d^3\mathbf{x}. \quad (12)$$

Average DW velocity is (see the Supplemental Materials [26] for detailed derivation),

$$\bar{v} = c_1 H + \frac{c_1}{\alpha_{\text{eff}}^2} \left(H - \sqrt{H^2 - H_W^2} \right) \quad (13)$$

where $c_1 = \frac{\alpha_{\text{eff}} \gamma_{\text{eff}}}{2S(1 + \alpha_{\text{eff}}^2)} \int \sin^2 \theta d^3\mathbf{x} = \frac{(M_1 - M_2)\alpha \bar{\Delta}}{(s_1 - s_2)^2 + \alpha^2}$ is peaked at the AMCP. Equation (13) is exact under very sensible assumptions, and all coefficients in Eq. (13) are fully determined by the model parameters.

Equation (13) predicts a negative differential DW mobility in the range of $H_W < H < \frac{\alpha_{\text{eff}}^2 + 1}{\sqrt{\alpha_{\text{eff}}^4 + 2\alpha_{\text{eff}}^2}} H_W$. This prediction is also true for ferromagnetic case. In order to find out how accurate of Eq. (13) is for $H > H_W$, we use MuMax3 [35] to numerically solve Eq. (2) for a synthetic ferrimagnetic strip wire as shown in Fig. 1 that consist of two antiferromagnetically-coupled ferromagnetic-layers of 1nm thick each. The strip size is 16 nm \times 2 nm \times 1024 nm. The cell size in simulations is chosen to be 1 nm \times 1 nm \times 1 nm. To mimic a GdFeCo alloy [9], the model parameters are $J = 1.2 \times 10^{-4} \text{ J} \cdot \text{A}^{-2} \text{m}^{-1}$, $A_1 = 9.8 \times 10^{-24} \text{ J} \cdot \text{m} \cdot \text{A}^{-2}$, $A_2 = 1.23 \times 10^{-23} \text{ J} \cdot \text{m} \cdot \text{A}^{-2}$, biaxial anisotropy are considered for each sublattice, $f_i = -\frac{K_{z,i}}{M_i^2} M_{i,z}^2 + \frac{K_{y,i}}{M_i^2} M_{i,y}^2$, $i = 1, 2$, $K_{z,1} = K_{z,2} = 0.65 \text{ MJ/m}^3$, $\alpha_{12} = \alpha_{21} = 0$. $K_{y,i}$ and α_{ii} ($i = 1, 2$) are used for simulating different systems as labelled by Set 1-6 in Table I. The gyromagnetic ratios $\gamma_1 = \gamma_2 = 1.76 \times 10^{11} \text{ s}^{-1} \text{ T}^{-1}$, the saturation magnetizations are $M_1 = 1010 \text{ kA/m}$, $M_2 = 900 \text{ kA/m}$. The coupling field between two sublattices is of hundreds of Tesla to guarantee collinearity of two spin sublattices. Different from a natural ferromagnet, inter-sublattice coupling is

Data set	Set 1	Set 2	Set 3	Set 4	Set 5	Set 6
$K_{y,1}(\text{MJ}/\text{m}^3)$	0.05	0.035	0.02	0.1	0.1	0.1
$K_{y,2}(\text{MJ}/\text{m}^3)$	0.05	0.035	0.02	0.1	0.1	0.1
α_{11}	0.02	0.02	0.02	0.005	0.01	0.015
α_{22}	0.02	0.02	0.02	0.005	0.01	0.015
α_{eff}	0.3473	0.3473	0.3473	0.0868	0.1736	0.2605
$K_y(\text{MJ}/\text{m}^3)$	0.1	0.07	0.04	0.2	0.2	0.2
$\mu_0 H_W(\text{T})$	0.3157	0.2210	0.1263	0.1579	0.3157	0.4736
$\bar{\Delta}(\text{nm})$	3.85	3.87	3.89	3.79	3.75	3.79
$c_1(\mu_0 \cdot \text{m} \cdot \text{s}^{-1} \text{T}^{-1})$	210.00	211.13	212.34	57.48	111.37	162.69

TABLE I. $K_{y,1}$, $K_{y,2}$, α_{11} , and α_{22} are model parameters. α_{eff} , K_y , $\mu_0 H_W$, $\bar{\Delta}$, and c_1 are computed quantities.

along the y -direction in our synthetic ferrimagnet. In the simulation, a DW is first created at the center of nanowire, then a uniform magnetic field is applied in the $+\hat{z}$ direction. The velocity is obtained from the linear fit of time-evolution curve of the DW center (where $m_z = 0$). For high fields above Walker breakdown, the average velocities are obtained from data accumulated for more than 4 velocity oscillating periods.

We consider six different systems with various $K_{y,i}$ and α_{ii} ($i = 1, 2$). The detail values of the model parameters are given in Table I. Because of large speed difference, Fig. 2(a) plot \bar{v} vs. H for three systems with the same $\alpha_{ii} = 0.02$ and different $K_{y,i}$, label as Set 1, 2, 3. Figure 2(b) is the similar plots for three systems with the same $K_{y,i} = 0.1 \text{ MJ}/\text{m}^3$, but different α_{ii} , label as Set 4, 5, 6. The corresponding values of c_1 , α_{eff} , and H_W computed from this theory are also given in Table I. The perfect agreements between the simulation results (the symbols) and theoretical prediction (the solid curves) demonstrate that Eq. (13) is almost exact.

Discussion and Conclusion.— Before conclusion, we would like to make a few remarks. 1) The relationship between the instantaneous DW speed and the DW structure is exact that explains why our high-field DW speed formula without any fitting parameters agree perfectly with simulation results. 2) Since no collective-mode approximation is used, the theory is applicable to all types of DWs. 3) High DW speed is a result of the absence of Walker breakdown field at the AMCP. This explains the observed high DW speed of more than 1.5km/s at the AMCP although the mobility $\mu = \frac{(M_1 - M_2)\Delta}{\alpha}$ for $H < H_W$ itself is comparable to or even smaller than that for a ferromagnetic wire [36, 37].

In summary, a generic theory of field-driven DW motion in FiM wires is presented. A static DW cannot exist in a homogeneous ferrimagnetic nanowire when a uniform static magnetic field or any other external force creates an energy density difference between two domains separated by the DW. Spins in the DW must vary with time under the external magnetic field such that the system energy is dissipated due to the Gilbert damping. The dissipated energy must be compensated by the Zeeman energy released from moving the DW toward the domain with the higher energy density. High DW speed near the AMCP is the consequence of the absences of precessional torque and infinite high Walker breakdown field at the

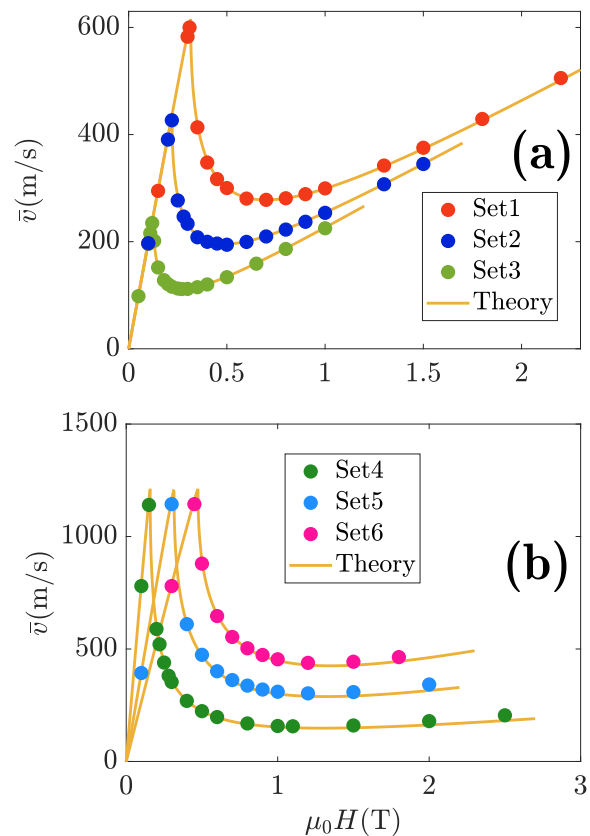


FIG. 2. Average DW speed of a head-to-head DW as a function of an applied field along the $+\hat{z}$ -direction. Symbols are MuMax3 simulation results and solid curves are theoretical formula without any fitting parameter. a) Three systems (denoted as Set 1, 2, 3) with the same $\alpha_{11} = \alpha_{22} = 0.02$ but different $K_{y,i}$. b) Three systems with (denoted as Set 4, 5, 6) with the same $K_{y,i} = 0.1 \text{ MJ}/\text{m}^3$ but different α_{ii} ($i = 1, 2$). Their values are listed in Table I.

AMCP. A lower Zeeman energy density and a high energy dissipation rate contribute also to the high DW speed at a reasonable lower field near the AMCP. Away from the AMCP, our approach can not only obtain the exact DW velocity below the Walker breakdown field, but also an almost exact velocity formula beyond the Walker breakdown field. This theory agrees

with all existing experiments and simulations, and provides useful guidances to DW manipulation.

Acknowledgments.— This work is supported by the National Key Research and Development Program of China 2020YFA0309600, the National Natural Science Foundation of China (Grant No. 11974296) and Hong Kong RGC Grants (No. 16301518, 16301619 and 6302321).

* Corresponding author: phxwan@ust.hk

- [1] B. Hu and X. R. Wang, Instability of Walker Propagating Domain Wall in Magnetic Nanowires, *Phys. Rev. Lett.* **111**, 027205 (2013).
- [2] X. S. Wang, P. Yan, Y. H. Shen, G. E. W. Bauer, and X. R. Wang, Domain Wall Propagation through Spin Wave Emission, *Phys. Rev. Lett.* **109**, 167209 (2012).
- [3] S. S. P. Parkin, M. Hayashi, L. Thomas, Magnetic Domain-Wall Racetrack Memory, *Science*, **320**, 190 (2008).
- [4] N. L. Schryer and L. R. Walker, The motion of 180° domain walls in uniform dc magnetic fields, *J. Appl. Phys.* **45**, 5406 (1974).
- [5] V. Baltz, A. Manchon, M. Tsoi, T. Moriyama, T. Ono, and Y. Tserkovnyak, Antiferromagnetic spintronics, *Rev. Mod. Phys.* **90**, 015005 (2018).
- [6] O. Gomonay, T. Jungwirth, and J. Sinova, High Antiferromagnetic Domain Wall Velocity Induced by Néel Spin-Orbit Torques, *Phys. Rev. Lett.* **117**, 017202 (2016).
- [7] S.-H. Yang, K.-S. Ryu, and S. Parkin, Domain-wall velocities of up to 750 m s⁻¹ driven by exchange-coupling torque in synthetic antiferromagnets, *Nat. Nanotechnol.* **10**, 221 (2015).
- [8] S. K. Kim, G. S. D. Beach, K.-J. Lee, T. Ono, T. Rasing, and Hyunsoo Yang, Ferrimagnetic spintronics, *Nat. Mater.* **21**, 24 (2022).
- [9] K.-J. Kim, S. K. Kim, Y. Hirata, S.-H. Oh, T. Tono, D.-H. Kim, T. Okuno, W. S. Ham, S. Kim, G. Go, Y. Tserkovnyak, A. Tsukamoto, T. Moriyama, K.-J. Lee, and T. Ono, Fast domain wall motion in the vicinity of the angular momentum compensation temperature of ferrimagnets, *Nat. Mater.* **16**, 1187 (2017).
- [10] L. Caretta, M. Mann, F. Büttner, K. Ueda, B. Pfau, C. M. Günther, P. Helsing, A. Churikova, C. Klose, M. Schneider, D. Engel, C. Marcus, D. Bono, K. Bagschik, S. Eisebitt, and G. S. D. Beach, Fast current-driven domain walls and small skyrmions in a compensated ferrimagnet, *Nat. Nanotechnol.* **13**, 1154 (2018).
- [11] S. A. Siddiqui, J. Han, J. T. Finley, C. A. Ross, and L. Liu, Current-Induced Domain Wall Motion in a Compensated Ferrimagnet, *Phys. Rev. Lett.* **121**, 057701 (2018).
- [12] T. Okuno, D.-H. Kim, S.-H. Oh, S. K. Kim, Y. Hirata, T. Nishimura, W. S. Ham, Y. Futakawa, H. Yoshikawa, A. Tsukamoto, Y. Tserkovnyak, Y. Shiota, T. Moriyama, K.-J. Kim, K.-J. Lee, and T. Ono, Spin-transfer torques for domain wall motion in antiferromagnetically coupled ferrimagnets, *Nat. Electron.* **2**, 389 (2019).
- [13] E. Haltz, J. Sampaio, S. Krishnia, L. Berges, R. Weil, and A. Mougin, Measurement of the tilt of a moving domain wall shows precession-free dynamics in compensated ferrimagnets, *Sci. Rep.* **10**, 16292 (2020).
- [14] D.-H. Kim, T. Okuno, S. K. Kim, S.-H. Oh, T. Nishimura, Y. Hirata, Y. Futakawa, H. Yoshikawa, A. Tsukamoto, Y. Tserkovnyak, Y. Shiota, T. Moriyama, K.-J. Kim, K.-J. Lee, and T. Ono, Low Magnetic Damping of Ferrimagnetic GdFeCo Alloys, *Phys. Rev. Lett.* **122**, 127203 (2019).
- [15] M. V. Logunov, S. S. Safonov, A. S. Fedorov, A. A. Danilova, N. V. Moiseev, A. R. Safin, S. A. Nikitov, and A. Kirilyuk, Domain Wall Motion Across Magnetic and Spin Compensation Points in Magnetic Garnets, *Phys. Rev. Applied* **15**, 064024 (2021).
- [16] V. V. Yurlov, K. A. Zvezdin, P. N. Skirdkov, and A. K. Zvezdin, Domain wall dynamics of ferrimagnets influenced by spin current near the angular momentum compensation temperature, *Phys. Rev. B* **103**, 134442 (2021).
- [17] W. H. Li, Z. Jin, D. L. Wen, X. M. Zhang, M. H. Qin, and J. M. Liu, Ultrafast domain wall motion in ferrimagnets induced by magnetic anisotropy gradient, *Phys. Rev. B* **101**, 024414 (2020).
- [18] M. Jin, I.-S. Hong, D.-H. Kim, K.-J. Lee, and S. K. Kim, Domain-wall motion driven by a rotating field in a ferrimagnet, *Phys. Rev. B* **104**, 184431 (2021).
- [19] S.-H. Oh, S. K. Kim, J. Xiao, and K.-J. Lee, Bidirectional spin-wave-driven domain wall motion in ferrimagnets, *Phys. Rev. B* **100**, 174403 (2019).
- [20] E. Haltz, S. Krishnia, L. Berges, A. Mougin, and J. Sampaio, Domain wall dynamics in antiferromagnetically coupled double-lattice systems, *Phys. Rev. B* **103**, 014444 (2021).
- [21] A. K. Zvezdin, Z. V. Gareeva, K. A. Zvezdin, Anomalies in the dynamics of ferrimagnets near the angular momentum compensation point, *J. Magn. Magn. Mater.* **509**, 166876 (2020).
- [22] E. Martínez, V. Raposo and Ó. Alejos, Novel interpretation of recent experiments on the dynamics of domain walls along ferrimagnetic strips, *J. Phys.: Condens. Matter* **32**, 465803 (2020).
- [23] A. A. Thiele, Steady-State Motion of Magnetic Domains, *Phys. Rev. Lett.* **30**, 230 (1973).
- [24] H. Y. Yuan, Q. Liu, K. Xia, Z. Yuan and X. R. Wang, Proper dissipative torques in antiferromagnetic dynamics, *Euro. Phys. Lett.* **126**, 67006 (2019).
- [25] A. Kamra, R. E. Troncoso, W. Belzig, and A. Brataas, Gilbert damping phenomenology for two-sublattice magnets, *Phys. Rev. B* **98**, 184402 (2018).
- [26] See Supplemental Materials at <https://journals.aps.org/prl/> for: 1) Energy dissipation rate and Rayleigh dissipation functional. 2) Detailed derivation of Eq. (3). 3) Illustration of three DW propagation modes. 4) Derivation of DW velocity formula Eq. (13). 5) Numerical verifications of excellent approximations used in the derivation of Eq. (13).
- [27] T. L. Gilbert, A phenomenological theory of damping in ferromagnetic materials, *IEEE Trans. Magn.* **40**, 3443 (2004).
- [28] R. K. Wangness, Sublattice Effects in Magnetic Resonance, *Phys. Rev.* **91**, 1085 (1953).
- [29] M. Binder, A. Weber, O. Mosendz, G. Woltersdorf, M. Izquierdo, I. Neudecker, J. R. Dahn, T. D. Hatchard, J.-U. Thiele, C. H. Back, and M. R. Scheinfein, Magnetization dynamics of the ferrimagnet CoGd near the compensation of magnetization and angular momentum, *Phys. Rev. B* **74**, 134404 (2006).
- [30] C. D. Stanciu, A. V. Kimel, F. Hansteen, A. Tsukamoto, A. Itoh, A. Kirilyuk, and T. Rasing, Ultrafast spin dynamics across compensation points in ferrimagnetic GdFeCo: The role of angular momentum compensation, *Phys. Rev. B* **73**, 220402(R) (2006).
- [31] Z. Z. Sun, X. R. Wang, Fast magnetization switching of Stoner particles: A nonlinear dynamics picture, *Phys. Rev. B* **71**, 174430 (2005).
- [32] Z. Z. Sun, X. R. Wang, Strategy to reduce minimal magnetization switching field for Stoner particles, *Phys. Rev. B* **73**,

- 092416 (2006).
- [33] X. R. Wang, P. Yan, J. Lu, and C. He, Magnetic field driven domain-wall propagation in magnetic nanowires, *Ann. Phys. (NY)*, **324**, 1815 (2009).
- [34] X. R. Wang, P. Yan, and J. Lu, High-field domain wall propagation velocity in magnetic nanowires, *Euro. Phys. Lett.* **86**, 67001 (2009).
- [35] A. Vansteenkiste, J. Leliaert, M. Dvornik, M. Helsen, F. G. Sanchez, and B. V. Waeyenberge, The design and verification of MuMax3, *AIP Advances* **4**, 107133 (2014).
- [36] T. Ono, H. Miyajima, K. Shigeto, K. Mibu, N. Hosoi, and T. Shinjo, Propagation of a Magnetic Domain Wall in a Submicrometer Magnetic Wire, *Science* **284**, 468 (1999).
- [37] G. S. D. Beach, C. Nistor, C. Knutson, M. Tsoi, and J. L. Erskine, Dynamics of field-driven domain-wall propagation in ferromagnetic nanowires, *Nat. Mater.* **4**, 741 (2005).